

## Nature of the Condensate in Mass Transport Models

Satya N. Majumdar,<sup>1</sup> M. R. Evans,<sup>2</sup> and R. K. P. Zia<sup>3</sup>

<sup>1</sup>*Laboratoire de Physique Théorique et Modèles Statistiques, Université Paris-Sud., Bât. 100. 91405 Orsay Cedex, France*

<sup>2</sup>*School of Physics, University of Edinburgh, Mayfield Road, Edinburgh, EH9 3JZ, United Kingdom*

<sup>3</sup>*Department of Physics and Center for Stochastic Processes in Science and Engineering, Virginia Tech, Blacksburg, Virginia 24061-0435, USA*

(Received 21 December 2004; published 11 May 2005)

We study the phenomenon of real space condensation in the steady state of a class of one-dimensional mass transport models. We derive the criterion for the occurrence of a condensation transition and analyze the precise nature of the shape and the size of the condensate in the condensed phase. We find two distinct condensate regimes: one where the condensate is Gaussian distributed and the particle number fluctuations scale normally as  $L^{1/2}$  where  $L$  is the system size, and the second regime where the particle number fluctuations become anomalously large and the condensate peak is non-Gaussian. We interpret these results within the framework of sums of random variables.

DOI: 10.1103/PhysRevLett.94.180601

PACS numbers: 05.40.-a, 02.50.Ey, 64.60.-i

Condensation transitions are ubiquitous in nature. For systems in thermal equilibrium, clustering is well understood in terms of the competition between entropy and energy (typically associated with attractive interactions). More exotic are condensations in systems with *no* interactions, e.g., Bose-Einstein's free (quantum) particles. Less understood are such transitions in *nonequilibrium* systems, in some of which even the concept of energy is dubious. For example, condensation is known to occur in many mass transport models, defined only by a set of rules of evolution, with no clear "attraction" between the masses [1–6]. The relevance of these models lies in their applicability to a broad variety of phenomena, e.g., traffic flow [7], force propagation through granular media [8], granular flow [9], and network dynamics [10]. Correspondingly, the condensation transition describes jamming in traffic [3], bunching of buses [5], clogging in pipes [5], coalescence of shaken steel balls [9], and condensation of edges in networks [10].

How such transitions arise is especially intriguing for one-dimensional ( $d = 1$ ) systems with *local* dynamical rules. A well-known example is the zero-range process (ZRP) [2,11,12] in which masses hop from site to (the next) site according to some transfer rule. In the steady state, a finite fraction of the total mass "condenses" onto a single site when  $\rho$ , the global mass density, is increased beyond a certain critical value:  $\rho_c$ . The system goes from a fluid phase, where the mass at each site hovers around  $\rho$ , to a condensed phase, where a fluid of density  $\rho_c$  coexists with a condensate containing all the "excess" mass.

Though condensation in these systems shares interesting analogies [3,6] with the traditional Bose-Einstein condensation, there are important differences. For example, here condensation occurs in real space and in all dimensions. Moreover these systems are *nonequilibrium* in the sense that they are defined by the dynamics, generally lack a Hamiltonian, and the stationary state is not specified by the usual Gibbs-Boltzmann distribution. There are two major

problems that one faces in the analysis of condensation in these systems. First, the stationary state itself often is very difficult to determine and secondly, even if it is known such as in ZRP, the analysis of condensation has so far been possible only within a grand canonical ensemble (GCE) where one is already in the thermodynamic ( $L \rightarrow \infty$ ) limit. While the GCE correctly predicts when a condensation transition can happen and even the value of the critical density  $\rho_c$ , it fails to provide much insight into the "condensed" phase ( $\rho > \rho_c$ ) itself. For that one needs to work in a canonical ensemble with the system size  $L$  finite, which has not been possible so far. In this Letter, we show that both of these problems can be overcome in a general class of mass transport models recently introduced by us [13]. This allows us to explore the condensed phase in detail revealing rather rich physical behaviors, in particular, the existence of two different types of condensates.

Our model is defined as follows: a mass  $m_i$  resides at each site  $i$  of a  $d = 1$  periodic lattice of size  $L$ . At each time step, a portion,  $\tilde{m}_i \leq m_i$ , chosen from a distribution  $\phi(\tilde{m}|m)$ , is chipped off to site  $i + 1$ . The dynamics conserves the total mass  $M = \sum_{i=1}^L m_i = \rho L$ . The model is general enough to include many previously studied models as special cases [13]. Choosing the chipping kernel  $\phi(\tilde{m}|m)$  appropriately recovers ZRP, the asymmetric random average process [14] and the chipping model of [6]. Moreover the model encompasses both discrete and continuous time dynamics and discrete and continuous mass. In particular, it was shown that the stationary state has a simple, factorized form provided the kernel is of the form  $\phi(\tilde{m}|m) \propto u(\tilde{m})v(m - \tilde{m})$  [13], where  $u(z)$  and  $v(z)$  are arbitrary non-negative functions. Then the joint distribution of mass in the steady state is given by

$$P(m_1, \dots, m_L) = \frac{\prod_{i=1}^L f(m_i)}{Z(M, L)} \delta\left(\sum_{j=1}^L m_j - M\right) \quad (1)$$

where  $f(m) = \int_0^m d\tilde{m} u(\tilde{m})v(m - \tilde{m})$  and the "canonical

partition function"  $Z(M, L)$  is just the normalization

$$Z(M, L) = \prod_{i=1}^L \int_0^\infty dm_i f(m_i) \delta\left(\sum_{j=1}^L m_j - M\right). \quad (2)$$

Note that (1) is a product of single-site weights  $f(m_i)$  but the delta function in (1) implies a fixed total mass thus inducing correlations between sites and in general the single-site mass *probability distribution*  $p(m) \neq f(m)$ .

The dynamics of the model specifies the functions  $u(\tilde{m})$  and  $v(m - \tilde{m})$ , which in turn specify the steady state uniquely in terms of weight function  $f(m)$ . Having determined the steady state, one next turns to the issue of condensation. In particular, we ask: (i) when does a condensation transition occur (ii) if condensation occurs, what is the precise nature of the condensate?

The factorization property allows (i) to be addressed rather easily within a GCE framework, a la Bose-Einstein. The approach implies taking the  $L \rightarrow \infty$  limit and setting the single-site mass distribution function  $p(m) = f(m)e^{-\mu m}$  where  $\mu$  is the chemical potential and is chosen to fix the density  $\rho = \int dm p(m)m$ . Thus, condensation must occur for  $\rho > \rho_c = \int dm f(m)m$  which is the maximum allowed value of  $\rho$  within the GCE. Based on previous works on the ZRP related case [4,5], it is easy to show that a condensation transition occurs if the single-site weights decay for large  $m$  as

$$f(m) \simeq Am^{-\gamma} \quad \text{with} \quad \gamma > 2. \quad (3)$$

A simple example of a chipping kernel which gives such weights is furnished by  $u(\tilde{m}) = \exp(-a\tilde{m})$  and  $v(m - \tilde{m}) = (1 + m - \tilde{m})^{-\gamma}$  which yield  $f(m) \simeq m^{-\gamma}/a$  for large  $m$ . In the following, we stay with the choice of  $f(m)$  in (3) and set, without loss of generality,  $\int_0^\infty f(m)dm = 1$ .

The GCE analysis correctly predicts the criterion for condensation and even the critical density  $\rho_c$ , but provides little insight into the condensed phase itself where  $\rho > \rho_c$ . In this work, we are able to explore the condensed phase by staying within the canonical ensemble and analyzing the mass distribution  $p(m) \equiv \int dm_2 \cdots dm_L P(m, \dots, m_L) \delta(\sum_{j=2}^L m_j + m - M)$  in a finite system of size  $L$ . Using (2), we have

$$p(m) = f(m) \frac{Z(M - m, L - 1)}{Z(M, L)}. \quad (4)$$

The rest of the Letter is devoted to the analysis of  $p(m)$  in (4) with  $f(m)$  given by (3). We have two parameters  $\gamma$  and  $\rho$ . Our goal is to show how the condensation is manifested by different behaviors of  $p(m)$  in different regions of the  $(\rho - \gamma)$  plane giving rise to a rich phase diagram in Fig. 2.

First, consider the Laplace transform of (2):

$$\int_0^\infty Z(M, L) e^{-sM} dM = [g(s)]^L, \quad (5)$$

where  $g(s) = \int_0^\infty f(m) e^{-sm} dm$ . The main challenge is to

invert (5) for a given  $f(m)$  and exploit its behavior to analyze  $p(m)$ . Before proceeding to the general case, let us present a case in which both  $Z(M, L)$  and  $p(m)$  can be obtained in closed form. We choose  $f(m) = 2e^{-1/m} m^{-5/2} / \sqrt{\pi}$ , for which  $g(s) = (1 + 2s^{1/2})e^{-2s^{1/2}}$  and our results below show that  $\rho_c = -g'(0) = 2$ . Now, (5) can be inverted to provide the closed form [15]:

$$Z(M, L) = B_{M,L} \left[ H_L(r) - \sqrt{M} H_{L-1}(r) \right], \quad (6)$$

where  $B_{M,L} = LM^{-(L+3)/2} e^{-L^2/M} / \sqrt{\pi}$ ,  $r = (2L + M)/2\sqrt{M}$  and  $H_k(r)$  is the Hermite polynomial of degree  $k$ . Substituting  $Z(M, L)$  in (4), we obtain  $p(m)$  explicitly and plot the case of  $L = 100$  in Fig. 1. The transition from the subcritical ( $\rho = 1$ ), through the critical ( $\rho = 2$ ), to the supercritical ( $\rho = 6$ ) cases, is clearly seen: the condensate showing up as an additional, asymmetric bump for  $\rho = 6$ . The explicit solution in this toy example provides us with useful insights into what to expect in the general case.

Before proceeding, let us summarize here our main results: we refer to Fig. 1 for typical forms of the mass distribution  $p(m)$  and Fig. 2 for a schematic phase diagram. In the subcritical regime the system is in a fluid phase where the mass distribution decays exponentially with decay length increasing with density. At  $\rho_c$  the distribution decays as a power law  $p(m) \sim m^{-\gamma}$  and at  $\rho > \rho_c$  the distribution develops an extra piece, representing the condensate, centered around  $M - L\rho_c$ . By our analysis within the canonical ensemble we show that this piece will have a "normal," Gaussian form when  $\gamma > 3$ . When  $\gamma < 3$ , however, the condensate will have an anomalous, asymmetric form as seen in Fig. 1 for  $\rho = 6$ . In the following we supply explicit expressions for these forms.

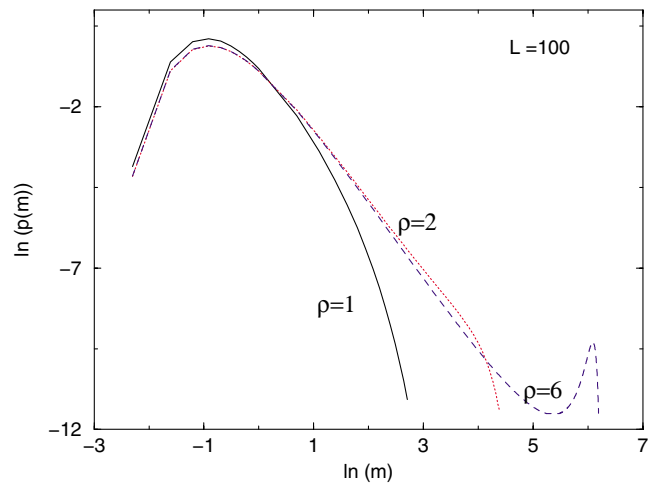


FIG. 1 (color online). The distribution  $p(m)$  vs  $m$  for the exactly solvable case, plotted using *Mathematica* for  $L = 100$  and  $\rho = 1$  (subcritical),  $\rho = \rho_c = 2$  (critical) and  $\rho = 6$  (supercritical). The condensate shows up as an additional bump near the tail of  $p(m)$  in the supercritical case.

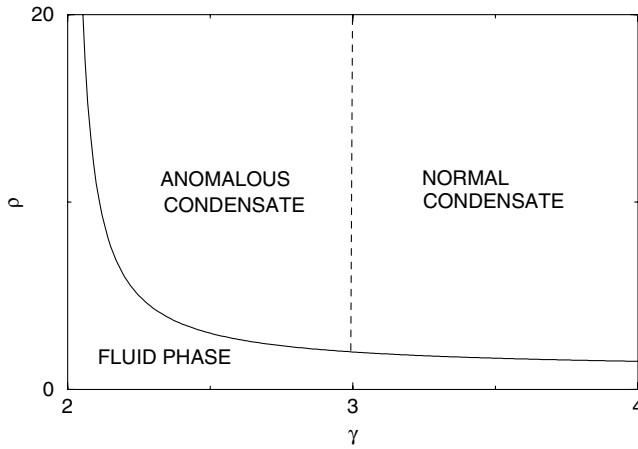


FIG. 2. Schematic phase diagram in the  $\rho - \gamma$  plane. The solid line represents the critical density  $\rho_c(\gamma)$ .

We formally invert (5) using the Bromwich formula,

$$Z(M, L) = \int_{s_0 - i\infty}^{s_0 + i\infty} \frac{ds}{2\pi i} \exp\left\{L[\ln g(s) + \rho s]\right\} \quad (7)$$

where the contour parallels the imaginary axis with its real part,  $s_0$ , to the right of all singularities of the integrand. Since  $f(m < 0) \equiv 0$ , the integrand is analytic in the right half plane. Therefore,  $s_0$  can assume any non-negative value. Meanwhile, for  $f$  given by (3),  $s = 0$  is a branch point singularity. As we shall see, in the subcritical case there exists a saddle point at positive  $s$  and  $s_0$  can be chosen to be this saddle point, whereas in the critical and supercritical cases the leading contribution is obtained by wrapping the contour around  $s = 0$ .

First we evaluate (7) in the limit  $L \rightarrow \infty$  by the saddle-point method, assuming it exists. Let  $h(s) \equiv \rho s + \ln g(s)$ . Then the saddle-point equation,  $h'(s_0) = 0$ , is

$$\rho = -g'(s_0)/g(s_0) = \rho(s_0) \quad (8)$$

leading us to, e.g.,

$$Z(M, L) \simeq \frac{\exp[Lh(s_0)]}{\sqrt{2\pi L h''(s_0)}}. \quad (9)$$

If  $\rho < \rho_c \equiv \rho(0)$ , then (8) has a solution for  $s_0 > 0$ , the saddle-point approximation is valid, no condensation occurs. Substituting (9) in (4) we get, for  $\rho < \rho_c$  and  $m \ll (\rho_c - \rho)L$ ,  $p(m) \simeq f(m)e^{-s_0 m}$ , recovering the GCE upon identifying the chemical potential  $\mu = s_0$ .

We now focus on the behavior as we approach criticality from the *subcritical* regime and consider (8) for small and positive  $\rho_c - \rho$ , i.e., small  $s_0$ . Thus, we just need the small  $s$  behavior of  $h(s)$ . For  $f(m)$  in (3) with a noninteger  $\gamma$ , one can expand, quite generally, the Laplace transform  $g(s)$  of (3) for small  $s$ , as

$$g(s) = \sum_{k=0}^{n-1} (-1)^k \frac{\mu_k}{k!} s^k + b s^{\gamma-1} + \dots \quad (10)$$

Here  $n = \text{int}[\gamma]$ ,  $\mu_k$  is the  $k$ th moment of  $f(m)$  (which exists for  $k < n$ ). The second term of (10) is the leading singular part and it can be shown that  $b = A\Gamma(1 - \gamma)$ . Note that  $\mu_0 = 1$  for normalized  $f$ ,  $\mu_1 = -g'(0) = \rho_c$  and  $\Delta \equiv \sqrt{\mu_2 - \mu_1^2}$ , which is the width of the distribution  $f$ , is finite if  $\gamma > 3$ . The role of  $\gamma = 3$  is now clear. The next-to-leading term is  $s^2$  in one case and  $s^{\gamma-1}$  in the other, so that the solution in (8) is given by  $s_0 \simeq (\rho_c - \rho)/\Delta^2$  for  $\gamma > 3$  and  $s_0 \simeq [(\rho_c - \rho)/b(\gamma - 1)]^{1/(\gamma-2)}$  otherwise. Inserting this behavior in the expression (9) gives for  $\gamma > 3$ ,  $Z(M, L) \sim \exp[-L(\rho_c - \rho)^2/2\Delta^2]$ , pointing to a system with Gaussian distributions and normal fluctuations. In contrast, for  $2 < \gamma < 3$ , we will show that anomalous fluctuations and non-Gaussians appear.

For the *supercritical* regime ( $\rho > \rho_c$ ), there is no solution to (8) on the positive real axis and more care is needed to find the asymptotic form of  $Z(M, L)$ . Our approach is to use the fact that the integral (7) will be dominated by  $s \simeq 0$ . Thus we can use the small  $s$  expansion (10) and develop a scaling analysis by identifying the different scaling regimes and calculating the corresponding scaling forms for  $Z(M, L)$  in the large  $L$  limit.

Using (10), one can rewrite (4) as

$$p(m) \simeq f(m) \frac{W[(m - M_{\text{ex}})/L]}{W(\rho_c - \rho)}, \quad (11)$$

where

$$W(y) = \int_{-i\infty}^{i\infty} \frac{ds}{2\pi i} \exp\left[L\left(-ys + \frac{\Delta^2}{2}s^2 + \dots + bs^{\gamma-1}\right)\right]$$

and  $M_{\text{ex}} \equiv (\rho - \rho_c)L$  is the excess mass. All crucial information about the condensate ‘‘bump’’ is encoded in the asymptotic behavior of  $W$ . Deferring the details to a later publication [15], we outline our main results below. Again, we consider the two cases ( $\gamma >$  or  $< 3$ ) separately.

Case I ( $\gamma > 3$ ): We find that, for large  $L$ , and in the  $O(L^{1/2})$  neighborhood of  $M_{\text{ex}}$ , the condensate appears in  $p(m)$  as a pure Gaussian and can be cast in scaling form:

$$p_{\text{cond}}(m) \simeq \frac{1}{\sqrt{2\pi L^3 \Delta}} e^{-z^2/2}; \quad z \equiv \frac{m - M_{\text{ex}}}{\Delta L^{1/2}}. \quad (12)$$

Note that its integral over  $m$  is  $1/L$ , indicating that the condensation occurs at a single site.

Case II ( $2 < \gamma < 3$ ): In the neighborhood of the excess mass  $M_{\text{ex}}$ , we find that  $p(m)$  has the scaling form:

$$p_{\text{cond}}(m) \simeq L^{-\gamma/(\gamma-1)} V_\gamma \left[ \frac{m - M_{\text{ex}}}{L^{1/(\gamma-1)}} \right]. \quad (13)$$

where  $V_\gamma(z) = \int_{-i\infty}^{i\infty} \frac{ds}{2\pi i} e^{-zs + bs^{\gamma-1}}$ . Though we have no closed form for  $V_\gamma(z)$ , we obtain its asymptotics:

$$V_\gamma(z) \simeq A|z|^{-\gamma} \quad \text{as } z \rightarrow -\infty \quad (14)$$

$$\simeq c_1 z^{(3-\gamma)/2(\gamma-2)} e^{-c_2 z^{(\gamma-1)/(\gamma-2)}} \quad \text{as } z \rightarrow \infty \quad (15)$$

where  $c_1, c_2$  are constants dependent on  $\gamma$ . Note that this

condensate bump is far from being Gaussian: it has a highly asymmetric shape, evidenced by (14) and (15). The peak occurs at  $m = M_{\text{ex}}$  and scales as  $\sim L^{-\gamma/(\gamma-1)}$ . Meanwhile its width is  $\gamma$  dependent:  $L^{1/(\gamma-1)}$ . The area under the bump is  $1/L$ , again implying that the condensate occurs at only one site.

Finally, in both Cases I and II the supercritical partition function is given by

$$Z(M, L) \sim AL/M_{\text{ex}}^\gamma. \quad (16)$$

Similar results for the critical case  $\rho = \rho_c$  and  $\gamma = 2, 3$  (where one obtains logarithmic corrections) will be published elsewhere [15].

The implication of these results are clear: in the condensed phase, the condensate acts as a reservoir for the critical fluid. Thus, the width of the condensate bump reflects the mass fluctuation in the critical fluid. For  $\gamma > 3$  we showed that condensate is Gaussian distributed with width  $\Delta L^{1/2}$ , so that the masses in the fluid fluctuate normally. For  $\gamma < 3$ , however, the width of the condensate and the mass fluctuations in the fluid are both anomalously large, namely,  $O(L^{1/(\gamma-1)})$ . Further implications concern the dynamics within the steady state. In systems with symmetry breaking, the ‘‘flip time’’  $\tau$  [16] is of interest. Here the translational symmetry is broken by the selection of a site to hold the condensate and  $\tau$  corresponds to the typical time a condensate exists before dissolving and reforming on another site. A rough estimate for  $\tau$  is  $p_{\text{cond}}^{-1}(m)$ , with  $|m - M_{\text{ex}}| \sim O(L)$ . For  $\gamma > 3$  this implies flip times growing exponentially with the system size, whereas for  $\gamma < 3$  they would diverge more slowly, as some power of  $L$ .

Our results may be naturally interpreted within the framework of sums of random variables. The partition function (2) gives the probability that the sum of  $L$  independent random variables  $m_i$ , each distributed according to  $f(m)$  is equal to  $M$ . Given  $f(m) \sim Am^{-\gamma}$  for large  $m$ ,  $Z(M, L)$  is just proportional to the probability distribution of the position of a Lévy walker (only taking positive steps) after  $L$  steps. Then (16) can be interpreted in terms of the extreme statistics of a Lévy walk. The mean of the sum is just  $\mu_1 L$ . Thus if  $M < L\mu_1 \equiv M_c$  one expects the sum to contain random variables of typical size  $O(1)$ , whereas for  $M > M_c$  one expects the sum to be dominated by a rare event, i.e.,  $L - 1$  of the variables would be of order  $O(\mu_1)$  except for one which would be large and equal to  $M - M_c$ . Given that  $f(m)$  is  $\sim Am^{-\gamma}$ , the probability that this large variable takes the value  $M - M_c$  is  $A(M - M_c)^{-\gamma}$ . This large contribution could be any of the  $L$  possible ones, thus the total probability is  $AL(M - M_c)^{-\gamma}$ , recovering (16). Moreover, the Gaussian  $L^{1/2}$  fluctuation for  $\gamma > 3$  and non-Gaussian  $L^{1/(\gamma-1)}$  fluctuation for  $2 < \gamma < 3$  correspond, respectively, to the normal and the anomalous diffusion of a Lévy process.

To summarize we have considered a very broad class of mass transport models and derived the condition for con-

densation. We have presented an analysis within the canonical ensemble that elucidates the nature and structure of the condensate. In particular we have identified two distinct condensate regimes where the condensate is normal and anomalous and derived the scaling distribution for the two types of condensate. Our results rely on the factorization property of the steady state (1), but we believe the phase scenario of Fig. 2 may apply in models without factorized steady states; it would be of interest to verify this. The underlying dynamics of the model we have studied are one-dimensional however the condition for a factorized state may be generalized to higher dimensions [15] and work is in progress to investigate condensation in such systems. Our results confirm that condensation may occur in a wider class of continuous mass models as well as discrete mass models such as the ZRP, as suggested in [17]. It would also be of interest to use this class of models to generalize the phase separation criterion of [18] which is based on the ZRP condensation.

This research is supported in part by the US NSF through DMR-0088451 and DMR-0414122.

- 
- [1] B. Schmittmann, K. Hwang, and R. K. P. Zia, *Europhys. Lett.* **19**, 19 (1992).
  - [2] M. R. Evans, *Braz. J. Phys.* **30**, 42 (2000).
  - [3] M. R. Evans, *Europhys. Lett.* **36**, 13 (1996).
  - [4] P. Bialas, Z. Burda, and D. Johnston, *Nucl. Phys.* **B493**, 505 (1997).
  - [5] O. J. O’Loan, M. R. Evans, and M. E. Cates, *Phys. Rev. E* **58**, 1404 (1998).
  - [6] S. N. Majumdar, S. Krishnamurthy, and M. Barma, *Phys. Rev. Lett.* **81**, 3691 (1998).
  - [7] D. Chowdhury, L. Santen, and A. Schadschneider, *Phys. Rep.* **329**, 199 (2000).
  - [8] S. N. Coppersmith, C.-h. Liu, S. Majumdar, O. Narayan, and T. A. Witten, *Phys. Rev. E* **53**, 4673 (1996).
  - [9] D. van der Meer *et al.*, *J. Stat. Mech. Theor. Exp.* **04** (2004) P04004; J. Torok, *cond-mat/0407567*.
  - [10] S. N. Dorogovtsev and J. F. F. Mendes, *Evolution of Networks* (OUP, Oxford, 2003).
  - [11] S. Großkinsky, G. M. Schütz, and H. Spohn, *J. Stat. Phys.* **113**, 389 (2003).
  - [12] C. Godrèche, *J. Phys. A* **36**, 6313 (2003).
  - [13] M. R. Evans, S. N. Majumdar, and R. K. P. Zia, *J. Phys. A* **37**, L275 (2004); R. K. P. Zia, M. R. Evans, and S. N. Majumdar, *J. Stat. Mech. Theor. Exp.* **10** (2004) L10001.
  - [14] J. Krug and J. Garcia, *J. Stat. Phys.* **99**, 31 (2000); R. Rajesh and S. N. Majumdar, *J. Stat. Phys.* **99**, 943 (2000).
  - [15] M. R. Evans, S. N. Majumdar, and R. K. P. Zia (unpublished).
  - [16] M. R. Evans, D. P. Foster, C. Godrèche, and D. Mukamel, *Phys. Rev. Lett.* **74**, 208 (1995).
  - [17] F. Zielen and A. Schadschneider, *Phys. Rev. Lett.* **89**, 090601 (2002).
  - [18] Y. Kafri, E. Levine, D. Mukamel, G. M. Schütz, and J. Török, *Phys. Rev. Lett.* **89**, 035702 (2002).